Robotica (2012) volume 30, pp. 333–342. © Cambridge University Press 2011
doi:10.1017/S0263574711000634

Unified analysis of statics of some limited-DOF parallel manipulators

Bo Hu†, Yi Lu†*, Xiuli Zhang‡ and Jianping Yu§

†*College of Mechanical Engineering, Yanshan University, Qinhuangdao, Hebei, 066004, P. R. China*
‡*College of Qinhuangdao Building Material, Qinhuangdao, Hebei, 066004 P. R.China*
§*College of Foreign Studies, Yanshan University, Qinhuangdao, Hebei, 066004, P. R. China*

(Received in Final Form: May 26, 2011; accepted May 24, 2011. First published online: July 1, 2011)

SUMMARY
An observation approach is proposed for determining the poses of the active/constrained wrench and the unified statics of some limited-DOF parallel manipulators (PMs) are studied systematically. First, a general PM model is constructed, and the unified inverse displacement is analyzed. Second, various types of acceptable legs are synthesized; the poses of the active/constrained wrench exerted on the various acceptable legs are determined by the observation approach. Third, a unified 6 × 6 Jacobina matrix and a unified statics equation are derived for solving active/constrained wrench of many limited-DOF PMs. Finally, two PMs are presented to illustrate this approach.

KEYWORDS: Parallel manipulators; Robot dynamics; Kinematics; Statics; Constraint wrench.

Nomenclatures

B, m	base and platform
r_i	active limb and its length ($i = 1, 2, \ldots, n$)
l_i, L_i	sides of m and B
P, R	prismatic joint and the revolute joint
U, S	universal joint and spherical joint
o, O	center point of m and B
a_i, A_i	vertices of m and B
e, E	the distances from a_i to o and from A_i to O
$\{m\}$	coordinate o-xyz fixed on m
$\{B\}$	coordinate O-XYZ fixed on B
$\boldsymbol{F}$	concentrated force exerted on m at o
$\boldsymbol{T}$	concentrated torque exerted on m at o
n	the number of independent pose parameters of m
θ_i	independent pose parameters of m
$\boldsymbol{F}_{ai}, \boldsymbol{T}_{ai}$	active forces and active torques exerted on r_i
$\boldsymbol{F}_{cj}, \boldsymbol{T}_{ck}$	constrained forces and torques exerted on r_j
x_l, x_m, x_n	direction cosine between x and X, x and Y, x and Z
y_l, y_m, y_n	direction cosine between y and X, y and Y, y and Z
z_l, z_m, z_n	direction cosine between z and X, z and Y, z and Z
α, β, γ	Euler angles of m about (X_a, Y_1, X_2), respectively
X_o, Y_o, Z_o	the position components of o in B_A
M	the number of degree of freedom
$\boldsymbol{\delta}_i, \boldsymbol{\tau}_i$	the unit vector of $\boldsymbol{F}_{ai}$ and $\boldsymbol{T}_{ai}$
$\boldsymbol{c}_j, \boldsymbol{t}_k$	the unit vector of $\boldsymbol{F}_{cj}$ and $\boldsymbol{T}_{ck}$
$\parallel, \perp$	parallel constraint and perpendicular constraint
b	$3^{1/2}$

* Corresponding author. E-mail: luyi@ysu.edu.cn

1. Introduction

Some limited-DOF (degree of freedom) parallel manipulators (PMs) have attracted much attention due to their relative high stiffness, simple structure, easy to control and have been used in many practical applications.[1–8] In order to determine the stress and precision and to select proper actuators, their active/constrained wrench must be solved.[1–3] In dynamics analysis, Huang *et al.*[2] solved the active forces of some PMs by the virtual parallel mechanism. Lu *et al.*[3] solved active forces of some limited-DOF PMs by a virtual serial mechanism and the principle of virtual work. Dasgupta and Mruthyunjaya[4] proposed a Newton–Euler formulation approach for the inverse dynamics of PMs. Tsai[5] solved the inverse dynamics of a Stewart–Gough PM by principle of virtual work. Gallardo *et al.*[6] analyzed dynamics of PMs by screw theory. On the basis of a Stewart platform, Dai and Huang[7] studied mobility of some over constrained PMs. Zhao *et al.*[8] studied the statics of some PMs by combining screw theory with virtual power theory. Di Gregorio[9] studied statics of a 3-UPU PM with three rotations. Kong and Gosselin[10] determined the pose of constrained wrench of some PMs using screw theory. Lu and Hu solved active/constrained forces of some PMs using Newton–Euler formulation approach and CAD variation geometry.[11–13] Zhao and Dai *et al.*[14–17] studied the kinematics/dynamics of PMs using the approach of the geometry and constraint analysis. Other researchers[18–25] studied the kinematics/dynamics of PMs using the vector analytic approach and Lagrange equations. Although each of these approaches has its merits, they are relative complicated and not easily to apply to solve the constrained wrench of some limited-DOF PMs with redundant and/or common constraints. Therefore, it is a significant issue to develop a simple, intuition and easily to learn approach for solving constrained wrench of some limited-DOF PMs and analyzing their unified statics.

This paper focuses on an observation approach for determining the poses of the active/constrained wrench of various limited-DOF PMs and studies their unified statics. Two PMs are presented to illustrate this approach. The results of study show that the proposed approach is simple, intuition and easy to determine the poses of the various active/constrained wrenches and to solve active/constrained wrench of many limited-DOF PMs.

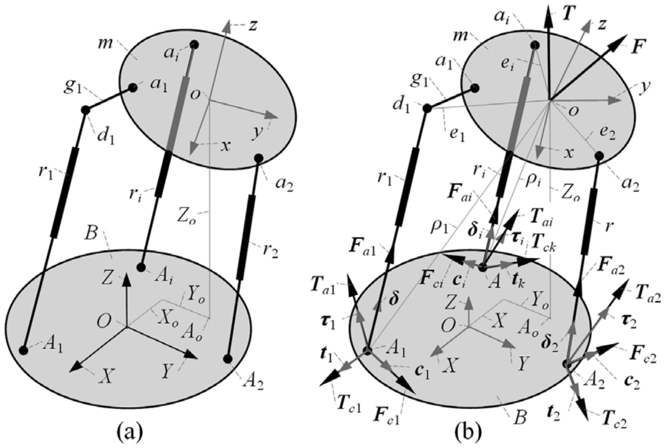

Fig. 1. A general PM with n active legs (a) and its force situation (b).

2. Common Technology for Solving Active/Constrained Wrench

2.1. A general PM and its inverse kinematics

A general PM with n linear/rotational actuators includes a fixed base B, a moving platform m, and n active limbs r_i $(i = 1, 2, \ldots, n)$, which connect m at a_i with B at A_i (see Fig. 1a). Each of active limbs r_i may be composed of a linear actuator or a rotational actuator. Each of active limbs r_i may be composed of some serial links connected by various joints. Let $\{m\}$ be a coordinate frame o-xyz fixed on m at o; $\{B\}$ be a coordinate frame O-XYZ fixed on B at O; $\|$ be a parallel constraint; and $\perp$ be a perpendicular constraint.

Before analyzing statics of PMs, the positions of the joints A_i on B and the joints a_i on m must be determined. The position vectors of A_i of B in $\{B\}$ are represented by $\boldsymbol{A}_i$ and the position vectors of $\boldsymbol{a}_i$ of m in $\{m\}$ and $\{B\}$ are represented by ${}^m\boldsymbol{a}_i$ and $\boldsymbol{a}_i$, respectively, as follows:[1,2]

$$\boldsymbol{A}_i = \begin{bmatrix} X_{Ai} \\ Y_{Ai} \\ Z_{Ai} \end{bmatrix}, \quad {}^m\boldsymbol{a}_i = \begin{bmatrix} x_{ai} \\ y_{ai} \\ z_{ai} \end{bmatrix}, \quad \boldsymbol{a}_i = \begin{bmatrix} X_{ai} \\ Y_{ai} \\ Z_{ai} \end{bmatrix}$$
$$\boldsymbol{R}_m^B = \begin{bmatrix} x_l & y_l & z_l \\ x_m & y_m & z_m \\ x_n & y_n & z_n \end{bmatrix}, \boldsymbol{o} = \begin{bmatrix} X_o \\ Y_o \\ Z_o \end{bmatrix}, \tag{1}$$
$$\boldsymbol{a}_i = \mathbf{R}_m^{B\,m}\boldsymbol{a}_i + \boldsymbol{o},$$

where $\boldsymbol{R}_m^B$ is a rotation transformation matrix from $\{m\}$ to $\{B\}$; $\boldsymbol{o}$ is a vector of point o on m in B; $(X_oY_oZ_o)$ are the components of $\boldsymbol{o}$. The constraint equations of $(x_l, x_m, x_n, y_l, y_m, y_n, z_l, z_m, z_n)$ in $\boldsymbol{R}_m^B$ can be obtained in refs. [1, 2]. When each of active legs $r_i (i = 1, 2, \ldots, n)$ of the PM is linear leg, r_i and its unit vector $\boldsymbol{\delta}_i$ and the vector $\boldsymbol{e}_i$ of the line e_i can be solved as follows:

$$r_i = |\boldsymbol{a}_i - \boldsymbol{A}_i|, \quad \boldsymbol{e}_i = \begin{bmatrix} e_{ix} \\ e_{iy} \\ e_{iz} \end{bmatrix} = \boldsymbol{a}_i - \boldsymbol{o},$$
$$\boldsymbol{\delta}_i = \begin{bmatrix} \delta_{ix} \\ \delta_{iy} \\ \delta_{iz} \end{bmatrix} = \frac{1}{r_i}\begin{bmatrix} X_{a_i} - X_{Ai} \\ Y_{a_i} - Y_{Ai} \\ Z_{a_i} - Z_{Ai} \end{bmatrix}. \tag{2}$$

When a active leg includes a link g_i and a linear active leg r_i, two ends of a link g_i are connected to platform m at a_i and to the one end of r_i at point d_i, respectively; and the other end of r_i is connected to the base B at point A_i. Thus, r_i, its unit vector $\boldsymbol{\delta}_i$, and the vector $\boldsymbol{e}_i$ of the line e_i can be solved as follows:

$$r_i = |\boldsymbol{d}_i - \boldsymbol{A}_i|, \quad \boldsymbol{\delta}_i = \frac{1}{r_i}\begin{bmatrix} X_{d_i} - X_{Ai} \\ Y_{d_i} - Y_{Ai} \\ Z_{d_i} - Z_{Ai} \end{bmatrix}, \quad \boldsymbol{e}_i = \boldsymbol{d}_i - \boldsymbol{o}. \tag{3}$$

Let α, β, γ be three Euler angles of m, and φ be one of α, β, γ. Set $s_\varphi = \sin\varphi$, $c_\varphi = \cos\varphi$, and $t_\varphi = \tan\varphi$. Let $\theta_i (i = 1, \ldots, n < 6)$ be n independent position-orientation parameters of the platform, $\theta_i \in (X_o, Y_o, Z_o, \alpha, \beta, \lambda)$. On the basis of the structure constraints of PMs, θ_i can be determined by the 6-n constrained equations. The extensions and the vectors $\boldsymbol{r}_i$ of active legs r_i, the unit vector $\boldsymbol{\delta}_i$ of $\boldsymbol{r}_i$, and the vector $\boldsymbol{e}_i$ can be represented by θ_i. Each of $(x_l, x_m, x_n, y_l, y_m, y_n, z_l, z_m, z_n)$ has been represented by (α, β, γ) in ref. [11] corresponding to the 12 different Euler rotational orders.

The inverse velocity $\boldsymbol{v}_{in}$ of limited-DOF PM can be expressed in ref. [11] as below

$$v_{in} = (\mathbf{J}_\alpha)_{n\times 6}\boldsymbol{V}, \quad \boldsymbol{v}_{in} = \begin{bmatrix} v_{r1} \\ \vdots \\ v_{rn} \end{bmatrix}_{n\times 1}, \quad \boldsymbol{V} = \begin{bmatrix} \boldsymbol{v} \\ \boldsymbol{\omega} \end{bmatrix}_{6\times 1}, \tag{4}$$

where $\mathbf{J}_\alpha$ is the $n \times 6$ Jacobian matrix, $\boldsymbol{V}$ is general velocity of m, and $\boldsymbol{v}$ and $\boldsymbol{\omega}$ are linear and angular velocities of m.

2.2. Active/constrained wrench of PMs

When ignoring the friction of all the joints in a PM, the whole workloads can be simplified as a wrench $(\boldsymbol{F}, \boldsymbol{T})$ applied onto m at the central point o. It includes the inertia wrench and the gravity of the platform, and inertia wrench and the gravity of the active legs, which can be mapped into a part of the whole workload, and the external working wrench (such as machining or operating wrench of tool, and damping wrench of end effector). $\boldsymbol{F}$ is a concentrated force and $\boldsymbol{T}$ is a concentrated torque. $(\boldsymbol{F}, \boldsymbol{T})$ are balanced by an active wrench $(\boldsymbol{F}_a, \boldsymbol{T}_a)$ and a constrained wrench $(\boldsymbol{F}_c, \boldsymbol{T}_c)$ (see Fig. 1b). Here, $\boldsymbol{F}_a$ includes n active wrenches $\boldsymbol{F}_{ai} (i = 1, \ldots, n)$, where $\boldsymbol{F}_{ai}$ can active force and torque, $\boldsymbol{F}_c$ includes n_2 constrained forces $\boldsymbol{F}_{cj} (j = 1, \ldots, n_1)$; $\boldsymbol{T}_c$ includes n_2 constrained torques $\boldsymbol{T}_{ck} (k = 1, \ldots, n_2)$. The equation $n_1 + n_2 + n = 6$ is satisfied.

In the limited-dof PMs, there are various possible active legs connected by various serial joints (see Table I). Some of them may be composed of some multi-DOF joints, such as spherical joint S, universal joint U, and cylindrical joint C. In order to determine the geometric constraints of the constrained wrench, an equivalent constrained leg r_e has to be constructed by replacing S with three uncoplanar and

https://doi.org/10.1017/S0263574711000634 Published online by Cambridge University Press

Table I. Possible serial structure of active leg for PMs.

Various possible serial structure of active legs				
UPU	UPRR	UPPP	UPC	UUR
URPR	URC	URU	UCP	CPU
CCR	CRRR	CRRP	CRPP	CRPR
RRPU	RRPRR	RRPPP	RRPC	RRUR
RRRPR	RRRC	RRRU	RRCP	PPPU
PPCR	PPRRR	PPRRP	PPRPP	PPRPR
RPPPP	RPPC	RPUR	RPUP	RPCR
RPRU	RPCP	PRPU	PRPRR	PRPPP
PRRRP	PRRPP	PRRPR	PRRC	PRRU
SRR	SRP	SPP	SPR	UPR
UUP	UCR	URRR	URRP	URPP
CPRR	CPPP	CPC	CUR	CUP
CRC	CRU	CCP	US	CS
RRUP	RRCR	RRRRR	RRRRP	RRRPP
PPPRR	PPPPP	PPPC	PPUR	PPUP
PPRC	PPRU	PPCP	RPPU	RPPRR
RPRRR	RPRRP	RPRPP	RPRPR	RPRC
PRPC	PRUR	PRUP	PRCR	PRRRR
PRCP	SU	SRR	SPP	SC
PRRR	RPU	PRU	RPRR	PRRR
RRPR	RRRP	PS	SP	

S-spherical joint, *U*-universal joint, *C*-cylindrical joint, *P*-prismatic joint, *R*-revolute joint

intersecting revolute joints, *U* with two crossed revolute joints, and *C* with a prismatic joint and a revolute joint, respectively.

Since the constrained wrench $(\boldsymbol{F}_c, \boldsymbol{T}_c)$ do not do any power during the movement of the PM, if there is $\boldsymbol{F}_c$, the following geometric constrains 1 and 2 must be satisfied. Otherwise, there is no $\boldsymbol{F}_c$. if there is $\boldsymbol{T}_c$, the following geometric constrain 3 must be satisfied. Otherwise, there is no $\boldsymbol{T}_c$. The three geometric constrains of $(\boldsymbol{F}_c, \boldsymbol{T}_c)$ can be determined by the observation approach as follows:

(1) Let $\boldsymbol{v}_{re}$ be a velocity along prismatic joint P in equivalent constrained leg r_e; thus, $\boldsymbol{F}_{cj}\boldsymbol{v}_{re} = 0$ must be satisfied, i.e. $\boldsymbol{F}_{cj} \perp P$. Thus, each of constrained forces $\boldsymbol{F}_{cj}$ must be perpendicular to all the prismatic joints in r_e.
(2) Let $\boldsymbol{R}_e$ be a unit vector of revolute joint R in r_e, and let $\boldsymbol{\rho}_r \times \boldsymbol{F}_{cj}$ be a torque of $\boldsymbol{F}_{cj}$ about R, $\boldsymbol{R}_e\,(\boldsymbol{\rho}_r \times \boldsymbol{F}_{cj}) = 0$ must be satisfied. Thus, each of constrained forces $\boldsymbol{F}_{cj}$ must intersect or be parallel with all the revolute joints in r_e. If active leg includes spherical joint S, $\boldsymbol{F}_{cj}$ must intersect with S.
(3) Let $\boldsymbol{\omega}_{re}$ be an angular velocity about R in r_e, $\boldsymbol{T}_{ck}\,\boldsymbol{\omega}_{re} = 0$ must be satisfied, i.e. $\boldsymbol{T}_{ck} \perp R$. Thus, each of constrained torques $\boldsymbol{T}_{ck}$ must be perpendicular to all the revolute joints in r_e.

Since the constrained force/torque do not do any work when movement of m, there are

$$F_{cj}\boldsymbol{c}_j \cdot \boldsymbol{v} + (F_{cj}\boldsymbol{\rho}_j \times \boldsymbol{c}_j)\cdot\boldsymbol{\omega} = 0 \quad (j = 1, \ldots, n_1), \tag{5}$$

$$T_{\tau k}\boldsymbol{\tau}_k \cdot \boldsymbol{\omega} = 0 \quad (k = 1, \ldots, n_2). \tag{6}$$

When F_{cj} and $T_{\tau k}$ are deleted from Eqs. (5) and (6), it leads to

$$\boldsymbol{0}_{(n_1+n_2)} = \mathbf{J}_c\boldsymbol{V}, \quad \mathbf{J}_c = \begin{bmatrix} \boldsymbol{c}_1^{\mathrm{T}} & (\boldsymbol{\rho}_1 \times \boldsymbol{c}_1)^{\mathrm{T}} \\ \vdots & \vdots \\ \boldsymbol{c}_{n1}^{\mathrm{T}} & (\boldsymbol{\rho}_{n1} \times \boldsymbol{c}_{n1})^{\mathrm{T}} \\ \boldsymbol{0}_{1\times 3} & \boldsymbol{c}_1^{\mathrm{T}} \\ \vdots & \vdots \\ \boldsymbol{0}_{1\times 3} & \boldsymbol{c}_{n2}^{\mathrm{T}} \end{bmatrix}, \tag{7a}$$

where $\mathbf{J}_c$ is a $(6-n)\times 6$ constrained wrench Jacobian matrix.

From Eqs. (4) and (7a), it leads to

$$\boldsymbol{v}_r = \mathbf{J}_{6\times 6}\boldsymbol{V}, \quad \boldsymbol{v}_r = \begin{bmatrix} \boldsymbol{v}_{in} \\ \boldsymbol{0}_{(6-n)\times 1} \end{bmatrix}, \quad \mathbf{J}_{6\times 6} = \begin{bmatrix} \mathbf{J}_\alpha \\ \mathbf{J}_c \end{bmatrix}. \tag{7b}$$

Let $\boldsymbol{F}_r = [F_{a_1}, \ldots, F_{an}F_{c_1}, \ldots, F_{cn_1}T_{\tau_1}, \ldots, T_{\tau n_2}]^{\mathrm{T}}$. On the basis of the principle of virtual work, it leads to

$$\boldsymbol{F}_r^{\mathrm{T}}\boldsymbol{v}_r + \begin{bmatrix} \boldsymbol{F} \\ \boldsymbol{T} \end{bmatrix}_{6\times 1}^{\mathrm{T}} \boldsymbol{V} = 0. \tag{8}$$

Substituting Eq. (7b) into Eq. (8), it leads to

$$\boldsymbol{F}_r = -\left(J_{6\times 6}^{-1}\right)^{\mathrm{T}} \begin{bmatrix} \boldsymbol{F} \\ \boldsymbol{T} \end{bmatrix}_{6\times 1}. \tag{9}$$

2.3. *Determination of pose of constrained wrench in some accepted active legs*

A key issue to solve the active/constrained wrenches is to determine their poses by the observation approach corresponding to different active legs. Some accepted active legs with linear/rotational actuator are constructed (see Fig. 2) for some 3-DOF PMs (such as 3SPR, 3RPS, 3RRPRR, 3UPU, 2UPU+SPR, 3UPRR, 3RPRU, 3RSR, and 3RPUR), for some 4-DOF PMs (such as 2UPS+2SPR, 2UPS+2UPU, 4UPU, 3SPU+UPR, 3SPU+SP, 3SPU+PRRR, and 3SPU+RPRR), and for some 5-DOF PMs (such as 4SPS+SPR, 4SPS+UPU, and 4SPS+URPR). When given the structure constraints of each accepted active leg, based on the three geometric constraints of $(\boldsymbol{F}_c, \boldsymbol{T}_c)$ in the Section 2.2, and the poses of active/constrained wrench in these accepted active legs can be determined by the observation approach (see Fig. 2). Here, R_j $(j = 1, 2, 3, 4)$ and $\boldsymbol{R}_j$ are the revolute joints and their unit vector; r is the extension of active leg r_i; $\boldsymbol{F}_a$ and $\boldsymbol{\delta}$ are an active force and its unit vector; $\boldsymbol{T}_a$ and $\boldsymbol{\tau}$ are an active torque and its unit vector; $\boldsymbol{F}_c$ and $\boldsymbol{c}$ are a constrained force and its unit vector; $\boldsymbol{T}_c$ and $\boldsymbol{t}$ are a constrained torque and its unit vector; $\boldsymbol{T}_r$ is a constrained torque produced by $\boldsymbol{F}_c$; a is the one end of active leg for connect with m; A is the other end of active leg for connect with B; g and $\boldsymbol{g}$ are an auxiliary link and its vector in $\{B\}$. When these accepted active legs are used to synthesize various

https://doi.org/10.1017/S0263574711000634 Published online by Cambridge University Press

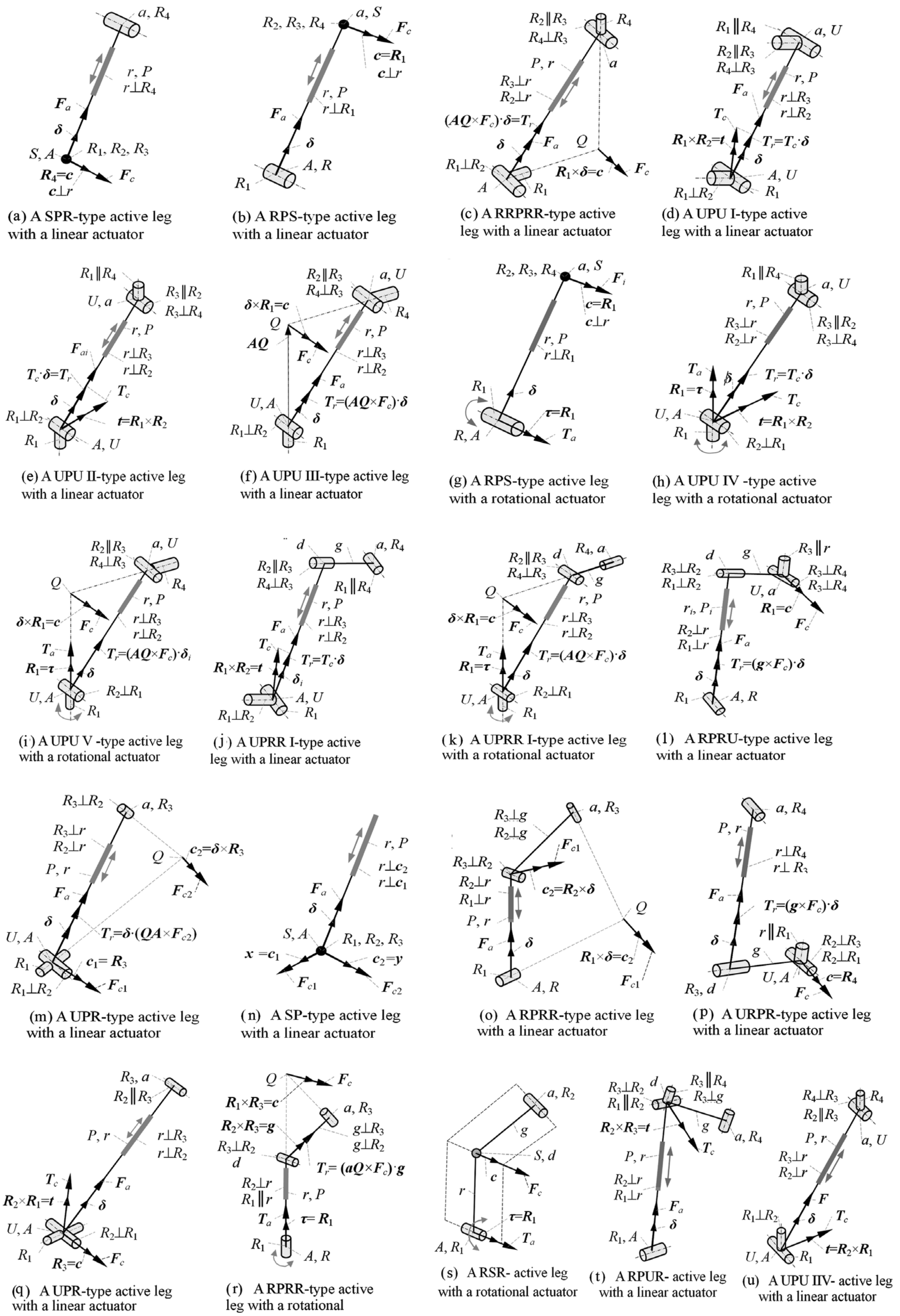

Fig. 2. Force situations of the 21 types active legs with given structure constraints.

https://doi.org/10.1017/S0263574711000634 Published online by Cambridge University Press

limited-DOF PMs, the active/constrained wrench of these PMs can be solved.

3. A 3RRPRR PM

3.1. The structure of the 3RRPRR PM and its geometric constraints

A 3RRPRR PM includes a moving platform m, a fixed base B, and 3 RRPRR-type active legs with the linear actuator (see Fig. 3a). Here, m is an equilateral ternary links with three vertices a_i ($i = 1, 2, 3$) and three sides l_i and a central point o; B is an equilateral ternary link with three vertices A_i and three sides L_i and a central point O. Each of RRPRR-type active legs connects m with B by two intercrossed revolute joints R_{3i} and R_{4i} at a_i, an active leg r_i with a prismatic joint P, and two intercrossed revolute joints R_{1i} and R_{2i} at A_i. In structure, some geometric constraints ($R_{1i} \perp R_{2i}$, R_{1i} coincident with a line A_iO, $R_{3i} \perp R_{4i}$, $R_{4i} \perp m$, $R_{2i} \perp r_i$, $R_{3i} \perp r_i$, and $R_{2i} \parallel R_{3i}$) are satisfied. Under these geometric constraints, the 3RRPRR PM has three planes $P_i(Oa_oa_iA_i)$, including r_i and a line a_oO, which is perpendicular to m at point a_o. Under the geometric constraints ($R_{3i} \perp a_oO$, $R_{2i} \parallel R_{3i}$, $R_{2i} \perp A_iO$, $R_{2i} \perp r_i$, and $R_{3i} \perp r_i$), some geometric constraints ($R_{2i} \perp \Delta a_oOa_i$, $R_{3i} \perp \Delta Oa_iA_i$, i.e., $R_{2i} \perp P_i$) are satisfied. Obviously, under these geometric constraints, $P_i \perp m$ is satisfied.

3.2. Inverse displacement kinematics

From Eq. (1), ${}^m\boldsymbol{a}_i$, $\boldsymbol{a}_i$ and $\boldsymbol{A}_i (i = 1, 2, 3)$ can be derived as follows:[11]

$$
\begin{aligned}
&{}^m\boldsymbol{a}_1 = \frac{e}{2}\begin{bmatrix} b \\ -1 \\ 0 \end{bmatrix}, {}^m\boldsymbol{a}_2 = \begin{bmatrix} 0 \\ e \\ 0 \end{bmatrix}, {}^m\boldsymbol{a}_3 = \frac{e}{2}\begin{bmatrix} -b \\ -1 \\ 0 \end{bmatrix}, \\
&\boldsymbol{A}_1 = \frac{E}{2}\begin{bmatrix} b \\ -1 \\ 0 \end{bmatrix}, \boldsymbol{A}_2 = \begin{bmatrix} 0 \\ E \\ 0 \end{bmatrix}, \boldsymbol{A}_3 = \frac{E}{2}\begin{bmatrix} -b \\ -1 \\ 0 \end{bmatrix}.
\end{aligned} \tag{10a}
$$

$$
\begin{aligned}
&\boldsymbol{a}_1 = \frac{1}{2}\begin{bmatrix} bex_l - ey_l + 2X_o \\ bex_m - ey_m + 2Y_o \\ bex_n - ey_n + 2Z_o \end{bmatrix}, \boldsymbol{a}_2 = \begin{bmatrix} ey_l + X_o \\ ey_m + Y_o \\ ey_n + Z_o \end{bmatrix}, \\
&\boldsymbol{a}_3 = \frac{1}{2}\begin{bmatrix} -bex_l - ey_l + 2X_o \\ -bex_m - ey_m + 2Y_o \\ -bex_n - ey_n + 2Z_o \end{bmatrix}.
\end{aligned} \tag{10b}
$$

where e is the distance from a_i to o ($i = 1, 2, 3$), E is the distance from A_i to O, and $b = 3^{1/2}$.

Corresponding to *XYX* rotational orders of the platform in ref. [11], $(x_l, x_m, x_n, y_l, y_m, y_n, z_l, z_m, z_n)$ can be represented by (α, β, γ) as follows:

$$
\begin{aligned}
&x_l = c_\beta, \quad x_m = s_\alpha s_\beta, \quad x_n = -c_\alpha s_\beta, \\
&y_l = s_\lambda s_\beta, \quad y_m = c_\alpha c_\lambda - s_\alpha c_\beta s_\lambda, \\
&y_n = s_\alpha c_\lambda + c_\alpha c_\beta s_\lambda, \quad z_l = c_\lambda s_\beta, \\
&z_m = -c_\alpha s_\lambda - s_\alpha c_\beta c_\lambda, \quad z_n = -s_\alpha s_\lambda + c_\alpha c_\beta c_\lambda.
\end{aligned} \tag{10c}
$$

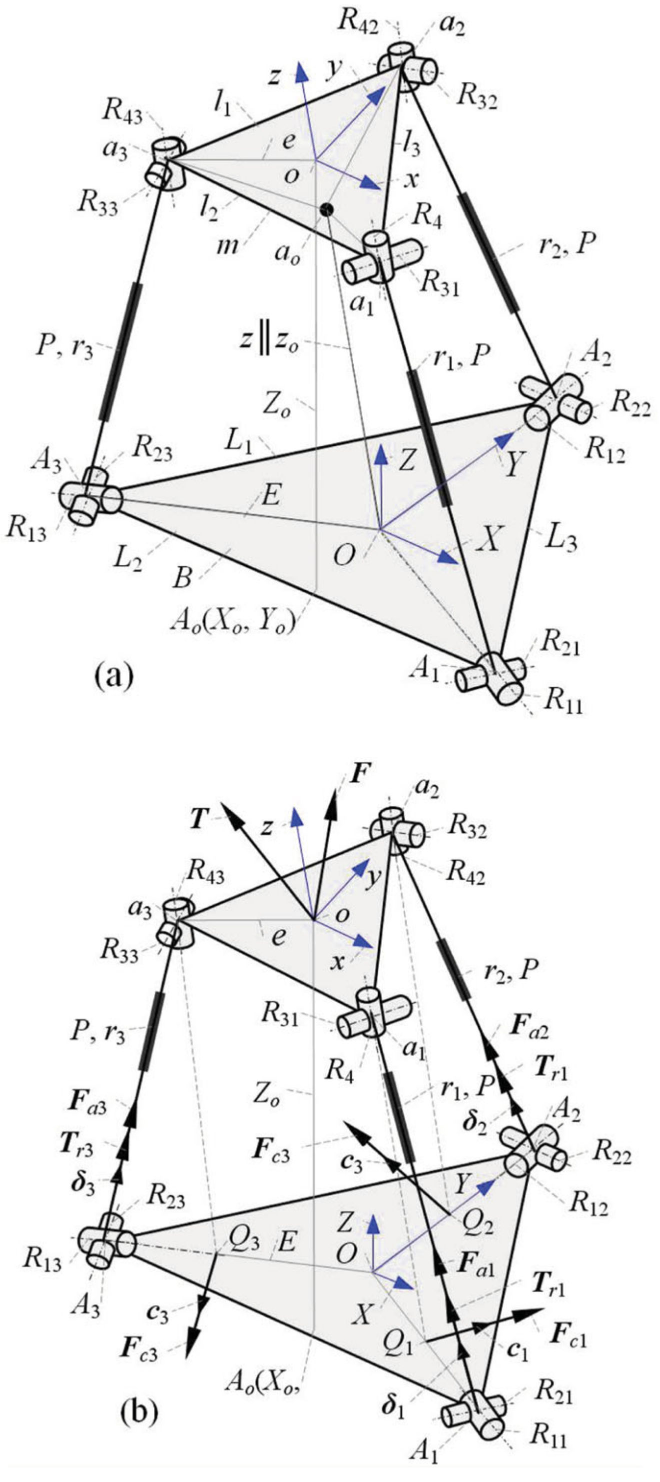

Fig. 3. (Colour online) The 3RRPRR PM and its force situation.

From $P_i \perp m$ ($i = 1, 2, 3$) of the 3RRPRR PM, the three equations of plane $P_i(Oa_oa_iA_i)$ are derived as follows:

$$
\begin{vmatrix} X_{A1} - X_{a1} & Y_{A1} - Y_{a1} & Z_{A1} - Z_{a1} \\ X_{a1} & Y_{a1} & Z_{a1} \\ z_l & z_m & z_n \end{vmatrix}
= \begin{vmatrix} \frac{e}{2}(bx_l - y_l) + X_o & \frac{e}{2}(bx_m - y_m) + Y_o & \frac{e}{2}(bx_n - y_n) + Z_o \\ bE/2 & -E/2 & 0 \\ z_l & z_m & z_n \end{vmatrix}
= 0,
$$

https://doi.org/10.1017/S0263574711000634 Published online by Cambridge University Press

$$\begin{vmatrix} X_{A2}-X_{a1} & Y_{A2}-Y_{a2} & Z_{A2}-Z_{a2} \\ X_{a2} & Y_{a2} & Z_{a2} \\ z_l & z_m & z_n \end{vmatrix} = \begin{vmatrix} ey_l+X_o & ey_m+Y & ey_n+Z_o \\ 0 & E & 0 \\ z_l & z_m & z_n \end{vmatrix} = 0,$$

$$\begin{vmatrix} X_{A3}-X_{a3} & Y_{A3}-Y_{a3} & Z_{A3}-Z_{a3} \\ X_{a3} & Y_{a3} & Z_{a3} \\ z_l & z_m & z_n \end{vmatrix} = \begin{vmatrix} -\frac{e}{2}(bx_l+y_l)+X_o & -\frac{e}{2}(bx_m+y_m)+Y_o & -\frac{e}{2}(bx_n+y_n)+Z_o \\ -bE/2 & -E/2 & 0 \\ z_l & z_m & z_n \end{vmatrix} = 0. \tag{11a}$$

Three plane equations are simplified as follows:

$$\begin{aligned} &be(z_nx_l-z_lx_n)-e(y_lz_n-z_ly_n) \\ &\quad +2X_oz_n-2Z_oz_l+3e(z_nx_m-z_mx_n) \\ &\quad +be(z_my_n-z_ny_m)+2b(Y_oz_n-Z_oz_m)=0, \\ &Z_oz_l-X_oz_n \\ &\quad = e(z_ny_l-y_lz_n)\times be(z_nx_l-z_lx_n)+e(y_lz_n-z_ly_n) \\ &\quad -2X_oz_n+2Z_oz_l-3e(z_nx_m-z_mx_n) \\ &\quad +be(z_my_n-z_ny_m)+2b(Y_oz_n-Z_oz_m)=0. \end{aligned} \tag{11b}$$

From Eqs. (2) and (11b), it leads to

$$\begin{aligned} &ey_m-ex_l+2Y_oz_n-2Z_oz_m=0,\ Z_oz_l-X_oz_n=-ex_m, \\ &ex_m-3ey_l+2X_oz_n-2Z_oz_l=0,\ x_m=y_l. \end{aligned} \tag{11c}$$

From Eqs. (2) and (11c), it leads to

$$\begin{aligned} &z_m^2=y_n^2,\quad z_l^2=x_n^2, \\ &X_o=\frac{Z_oz_l+rx_m}{z_n},\quad Y_o=\frac{2Z_oz_m+r(x_l-y_m)}{2z_n}. \end{aligned} \tag{11d}$$

From Eqs. (2) and (11c), it leads to $(-c_\alpha s_\beta)^2=(c_\gamma s_\beta)^2$, i.e, $\alpha=\gamma$. Next, from Eqs. (10c) and (11d), it leads to

$$\begin{aligned} X_o&=\frac{(Z_oc_\alpha+es_\alpha)s_\beta}{-s_\alpha^2+c_\alpha^2c_\beta}, \\ Y_o&=\frac{Z_os_\alpha c_\alpha(1+c_\beta)+e\left(c_\beta-c_\alpha^2+s_\alpha^2c_\beta\right)/2}{-s_\alpha^2+c_\alpha^2c_\beta}. \end{aligned} \tag{11e}$$

The formulae for solving r_i are derived from Eqs. (2), (3), (10), and (11) as follows:

$$\begin{aligned} r_2^2&=D+2e(y_lX_o+y_mY_o+y_nZ_o)-2E(ey_m+Y_o), \\ D&=X_o^2+Y_o^2+Z_o^2+E^2+e^2, \\ r_1^2&=D+EY_o-bEX_o+be(x_lX_o+x_mY_o+x_nZ_o) \\ &\quad -e(y_lX_o+y_mY_o+y_nZ_o) \\ &\quad +eE(by_l+bx_m-3x_l-y_m)/2, \\ r_3^2&=D+EY_o+bEX_o-be(x_lX_o+x_mY_o+x_nZ_o) \\ &\quad -e(y_lX_o+y_mY_o+y_nZ_o)-eE \\ &\quad \times(by_l+bx_m+3x_l+y_m)/2. \end{aligned} \tag{12}$$

When given (α,β,Z_o), $r_i(i=1,2,3)$ can be represented by (α,β,Z_o) from Eqs. (11e) and (12).

3.3. Active force and constrained force and torque

A loop equation of OA_ia_io can be expressed as

$$\boldsymbol{OA}_i+\boldsymbol{A}_i\boldsymbol{a}_i=\boldsymbol{Oo}+\boldsymbol{oa}_i. \tag{13a}$$

Differentiating both sides of Eq. (13a) with respect to time, it leads to

$$\begin{aligned} &v_{ri}\boldsymbol{\delta}_i+\boldsymbol{\omega}_{ri}\times r_i\boldsymbol{\delta}_i=\boldsymbol{v}+\boldsymbol{\omega}\times\boldsymbol{e}_i,\quad \boldsymbol{\delta}_i=\frac{\boldsymbol{a}_i-\boldsymbol{A}_i}{|\boldsymbol{a}_i-\boldsymbol{A}_i|}, \\ &\boldsymbol{e}_i=\boldsymbol{a}_i-\boldsymbol{o}, \end{aligned} \tag{13b}$$

where v_{ri} is the input velocity of r_i and $\boldsymbol{\omega}_{ri}$ is the angular velocity vector of r_i.

Dot multiplying both side of Eq. (13b) by $\boldsymbol{\delta}_i$, it leads to

$$\begin{aligned} &v_{ri}=\left[\boldsymbol{\delta}_i^{\mathrm{T}}\quad(\boldsymbol{e}_i\times\boldsymbol{\delta}_i)^{\mathrm{T}}\right]\boldsymbol{V}, \\ &\boldsymbol{v}_{in}=\mathbf{J}_\alpha\boldsymbol{V},\ \boldsymbol{v}_{in}=[v_{r1}\quad v_{r2}\quad v_{r3}]^{\mathrm{T}}. \end{aligned} \tag{13c}$$

On the basis of the force situation of the RRPRR-type active leg with a linear actuator, the force situation of the 3RRPRR PM is determined (see Fig. 3b). From Eqs. (7b), (9) and (13c), the active and constrained forces can be solved as follows:

$$\begin{aligned} &[F_{a1}\quad F_{a2}\quad F_{a3}\quad F_{c1}\quad F_{c2}\quad F_{c3}]^{\mathrm{T}}=-\left(\mathbf{J}_{6\times6}^{-1}\right)^{\mathrm{T}}\begin{bmatrix}\boldsymbol{F}\\ \boldsymbol{T}\end{bmatrix}_{6\times1}, \\ &\mathbf{J}_{6\times6}=\begin{bmatrix}\mathbf{J}_\alpha\\ \mathbf{J}_c\end{bmatrix},\quad \mathbf{J}_\alpha=\begin{bmatrix}\boldsymbol{\delta}_1^{\mathrm{T}} & (\boldsymbol{e}_1\times\boldsymbol{\delta}_1)^{\mathrm{T}}\\ \boldsymbol{\delta}_2^{\mathrm{T}} & (\boldsymbol{e}_2\times\boldsymbol{\delta}_2)^{\mathrm{T}}\\ \boldsymbol{\delta}_3^{\mathrm{T}} & (\boldsymbol{e}_3\times\boldsymbol{\delta}_3)^{\mathrm{T}}\end{bmatrix}, \\ &\mathbf{J}_c=\begin{bmatrix}\boldsymbol{c}_1^{\mathrm{T}} & (\boldsymbol{\rho}_1\times\boldsymbol{c}_1)^{\mathrm{T}}\\ \boldsymbol{c}_2^{\mathrm{T}} & (\boldsymbol{\rho}_2\times\boldsymbol{c}_2)^{\mathrm{T}}\\ \boldsymbol{c}_3^{\mathrm{T}} & (\boldsymbol{\rho}_3\times\boldsymbol{c}_3)^{\mathrm{T}}\end{bmatrix}. \end{aligned} \tag{13d}$$

Three constrained torques $\boldsymbol{T}_{ri}$ are solved as

$$\boldsymbol{T}_{ri}=[F_{ci}\boldsymbol{c}_i\times(\boldsymbol{A}_i-\boldsymbol{Q}_i)]\cdot\boldsymbol{\delta}_i. \tag{13e}$$

All relevant items in Eq. (13d) can be derived as follows:

From Eqs. (10c) and (11c), it leads to

$$\begin{aligned} &x_l=c_\beta,\quad x_m=s_\alpha s_\beta,\quad x_n=-c_\alpha s_\beta, \\ &y_l=s_\alpha s_\beta,\quad y_m=c_\alpha^2-s_\alpha^2c_\beta,\quad y_n=-s_\alpha c_\alpha(1+c_\beta), \\ &z_l=c_\alpha s_\beta,\quad z_m=s_\alpha c_\alpha(1+c_\beta),\quad z_n=-s_\alpha^2+c_\alpha^2c_\beta. \end{aligned} \tag{14a}$$

The unit vectors $\boldsymbol{R}_{ji}$ of revolute joints R_{ji} $(j=1,2,3,4;i=1,2,3)$ are determined as follows:

$$\begin{aligned} &\boldsymbol{R}_{11}=\frac{1}{2}\begin{bmatrix}b\\-1\\0\end{bmatrix},\quad \boldsymbol{R}_{12}=\begin{bmatrix}0\\1\\0\end{bmatrix},\quad \boldsymbol{R}_{13}=\frac{1}{2}\begin{bmatrix}-b\\-1\\0\end{bmatrix}, \\ &\boldsymbol{R}_{41}=\boldsymbol{R}_{42}=\boldsymbol{R}_{43}=\begin{bmatrix}z_l\\z_m\\z_n\end{bmatrix}, \\ &\boldsymbol{R}_{21}=\boldsymbol{R}_{31},\quad \boldsymbol{R}_{22}=\boldsymbol{R}_{32},\quad \boldsymbol{R}_{22}=\boldsymbol{R}_{32}. \end{aligned} \tag{14b}$$

https://doi.org/10.1017/S0263574711000634 Published online by Cambridge University Press

An equation of axis of R_{4i} is expressed as

$$(x - X_{ai})/z_l = (y - Y_{ai})/z_m = (z - Z_{ai})/z_n. \quad (14c)$$

When $z = 0$, from Eq. (14c), three intersected points Q_i of R_{4i} and OA_i in $\{B\}$ are derived as follows:

$$Q_1 = \frac{1}{z_n}\begin{bmatrix} -Z_{a1}z_l + X_{a1}z_n \\ -Z_{a1}z_m + Y_{a1}z_n \\ 0 \end{bmatrix} = \frac{1}{2z_n}\begin{bmatrix} -(bex_n - ey_n + 2Z_o)z_l + (bex_l - ey_l + 2X_o)z_n \\ -(bex_n - ey_n + 2Z_o)z_m + (bex_m - ey_m + 2Y_o)z_n \\ 0 \end{bmatrix},$$

$$Q_2 = \frac{1}{z_n}\begin{bmatrix} -Z_{a2}z_l + X_{a2}z_n \\ -Z_{a2}z_m + Y_{a2}z_n \\ 0 \end{bmatrix} = \frac{1}{z_n}\begin{bmatrix} -(ey_n + Z_o)z_l + (ey_l + X_o)z_n \\ -(ey_n + Z_o)z_m + (ey_m + Y_o)z_n \\ 0 \end{bmatrix},$$

$$Q_3 = \frac{1}{z_n}\begin{bmatrix} -Z_{a3}z_l + X_{a3}z_n \\ -Z_{a3}z_m + Y_{a3}z_n \\ 0 \end{bmatrix} = \frac{1}{2z_n}\begin{bmatrix} (bex_n + ey_n - 2Z_o)z_l + (-bex_l - ey_l + 2X_o)z_n \\ (bex_n + ey_n - 2Z_o)z_m + (-bex_m - ey_m + 2Y_o)z_n \\ 0 \end{bmatrix}. \quad (14d)$$

The unit vector $\boldsymbol{\delta}_i$ of r_i, the vector $\boldsymbol{e}_i$ of the line e_i, the unit vector $\boldsymbol{c}_i$ of constrained force $\boldsymbol{F}_{ci}$, and the arm vector $\boldsymbol{\rho}_i$ of $\boldsymbol{F}_{ci}$ to o can be solved as follows:

$$\boldsymbol{c}_i = \boldsymbol{R}_{2i} = \frac{\boldsymbol{R}_{1i} \times \boldsymbol{\delta}_i}{|\boldsymbol{R}_{1i} \times \boldsymbol{\delta}_i|}, \quad \boldsymbol{\rho}_i = \boldsymbol{Q}_i - \boldsymbol{o}, \quad (i = 1, 2, 3),$$

$$\boldsymbol{o} = \begin{bmatrix} \dfrac{Z_o c_\alpha s_\beta + r s_\alpha s_\beta}{-s_\alpha^2 + c_\alpha^2 c_\beta} \\ \dfrac{-Z_o c_\alpha s_\alpha (1 + c_\beta) + r\left(c_\beta - c_\alpha^2 + s_\alpha^2 c_\beta\right)/2}{-s_\alpha^2 + c_\alpha^2 c_\beta} \\ Z_o \end{bmatrix}. \quad (14e)$$

When given (α, β, Z_o), $\boldsymbol{o}$, $\boldsymbol{Q}_i$, $\boldsymbol{\delta}_i$, $\boldsymbol{e}_i$, $\boldsymbol{c}_i$, and $\boldsymbol{\rho}_i$ can be solved from Eqs. (11e), (12), (13b), and (14a)–(e).

4. The 2SPS+2SPR PM

4.1. The 2SPS+2SPR PM and its geometric constraints

A 2SPS+2SPR PM (see Fig. 4a) has 4 DOFs, i.e., $n = M = 4$. It includes a platform m, a base B, and four linear active legs $r_i (i = 1, 2, 3, 4)$ with linear actuator for connecting m with B. In order to avoid the singularity of mechanism, the shape of B and m should be a square and a rectangle, respectively. Here, two SPS-type limbs connect m at a_i with B at $A_i (i = 1, 4)$, and two SPR-type active limbs connect m at a_i with B at $A_i (i = 2, 3)$.

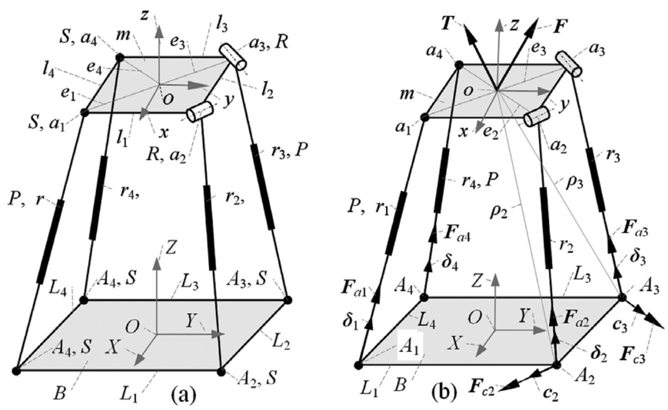

Fig. 4. The 2SPS+2SPR PM (a) and its forces situation (b).

4.2. Inverse displacement kinematics

From Eq. (2), ${}^m\boldsymbol{a}_i$, $\boldsymbol{A}_i$ and $\boldsymbol{a}_i (i = 1, 2, 3, 4)$ can be derived as follows:

$${}^m\boldsymbol{a}_1 = \frac{1}{2}\begin{bmatrix} l_1 \\ -l_2 \\ 0 \end{bmatrix}, \quad {}^m\boldsymbol{a}_2 = \frac{1}{2}\begin{bmatrix} l_1 \\ l_2 \\ 0 \end{bmatrix}, \quad {}^m\boldsymbol{a}_3 = \frac{1}{2}\begin{bmatrix} -l_1 \\ l_2 \\ 0 \end{bmatrix}, \quad {}^m\boldsymbol{a}_4 = \frac{1}{2}\begin{bmatrix} -l_1 \\ -l_2 \\ 0 \end{bmatrix},$$

$$\boldsymbol{A}_1 = \frac{L}{2}\begin{bmatrix} 1 \\ -1 \\ 0 \end{bmatrix}, \quad \boldsymbol{A}_2 = \frac{L}{2}\begin{bmatrix} 1 \\ 1 \\ 0 \end{bmatrix}, \quad \boldsymbol{A}_3 = \frac{L}{2}\begin{bmatrix} -1 \\ 1 \\ 0 \end{bmatrix}, \quad \boldsymbol{A}_4 = \frac{L}{2}\begin{bmatrix} -1 \\ -1 \\ 0 \end{bmatrix}, \quad (15a)$$

$$\boldsymbol{a}_1 = \frac{1}{2}\begin{bmatrix} x_l l_1 - y_l l_2 + 2X_o \\ x_m l_1 - y_m l_2 + 2Y_o \\ x_n l_1 - y_n l_2 + 2Z_o \end{bmatrix}, \quad \boldsymbol{a}_2 = \frac{1}{2}\begin{bmatrix} x_l l_1 + y_l l_2 + 2X_o \\ x_m l_1 + y_m l_2 + 2Y_o \\ x_n l_1 + y_n l_2 + 2Z_o \end{bmatrix},$$

$$\boldsymbol{a}_3 = \frac{1}{2}\begin{bmatrix} -x_l l_1 + y_l l_2 + 2X_o \\ -x_m l_1 + y_m l_2 + 2Y_o \\ -x_n l_1 + y_n c_2 + 2Z_o \end{bmatrix}, \quad \boldsymbol{a}_4 = \frac{1}{2}\begin{bmatrix} -x_l l_1 - y_l l_2 + 2X_o \\ -x_m l_1 - y_m l_2 + 2Y_o \\ -x_n l_1 - y_n l_2 + 2Z_o \end{bmatrix}. \quad (15b)$$

In the 2SPS+2SPR PM, there are two geometric constrains ($r_2 \perp e_1$ and $r_3 \perp e_2$). From them, two geometric constraint equations are derived as follows:

$$\boldsymbol{a}_2\boldsymbol{A}_2 \cdot \boldsymbol{a}_1\boldsymbol{a}_3 = \frac{1}{2}\begin{bmatrix} x_l l_1 + y_l l_2 + 2X_o - L \\ x_m l_1 + y_m l_2 + 2Y_o - L \\ x_n l_1 + y_n l_2 + 2Z_o \end{bmatrix}^{\mathrm{T}}\begin{bmatrix} x_l l_1 - y_l l_2 \\ x_m l_1 - y_m l_2 \\ x_n l_1 - y_n l_2 \end{bmatrix} = 0,$$

https://doi.org/10.1017/S0263574711000634 Published online by Cambridge University Press

$$\boldsymbol{a}_3\boldsymbol{A}_3 \cdot \boldsymbol{a}_2\boldsymbol{a}_4 = \frac{1}{2}\begin{bmatrix} -x_l l_1 + y_l l_2 + 2X_o + L \\ -x_m l_1 + y_m l_2 + 2Y_o - L \\ -x_n l_1 + y_n l_2 + 2Z_o \end{bmatrix}^{\mathrm{T}} \begin{bmatrix} x_l l_1 + y_l l_2 \\ x_m l_1 + y_m l_2 \\ x_n l_1 + y_n l_2 \end{bmatrix} = 0. \tag{16a}$$

From (16a), it leads to

$$\begin{gathered} l_1(X_o x_l + Y_o x_m + Z_o x_n) - E l_1 x_m + L l_2 y_l/2 = 0, \\ l_1^2 - L l_1 x_l - l_2^2 - 2l_2(X_o y_l + Y_o y_m + Z_o y_n) + L l_2 y_m = 0. \end{gathered} \tag{16b}$$

From (16b), it leads to

$$\begin{aligned} X_o &= \frac{1}{2}\left[\frac{l_2 x_m + 2Z_o z_l}{z_n} - \frac{L l_2 y_l y_m}{z_n l_1} - \frac{l_1 x_m (l_1 - L x_l)}{z_n l_2}\right], \\ Y_o &= \frac{1}{2}\left[\frac{2Z_o z_m - l_2 x_l}{z_n} + \frac{l_1 x_l (l_1 - 2E x_l)}{l_2 z_n} + \frac{L l_2 y_l^2}{l_1 z_n}\right] + E. \end{aligned} \tag{16c}$$

Corresponding to *XYX* rotational orders of the platform in ref. [10], $(x_l\ x_m\ x_n\ y_l\ y_m\ y_n\ z_l\ z_m\ z_n)$ can be represented by (α, β, γ) as the same as Eq. (10c). From Eqs. (10c) and (16c), it leads to

$$\begin{aligned} X_o &= \frac{s_\beta[l_2 s_\alpha + 2Z_o c_\lambda - L s_\lambda (c_\alpha c_\lambda - s_\alpha c_\beta s_\lambda)\frac{l_2}{l_1} - s_\alpha (l_1 - L c_\beta)\frac{l_1}{l_2}]}{2(c_\alpha c_\beta c_\lambda - s_\alpha s_\lambda)}, \\ Y_o &= \frac{-2Z_o(c_\alpha s_\lambda + s_\alpha c_\beta c_\lambda) - l_2 c_\beta + c_\beta (l_1 - L c_\beta)\frac{l_1}{l_2} + L s_\beta^2 s_\lambda^2 \frac{l_2}{l_1}}{2(c_\alpha c_\beta c_\lambda - s_\alpha s_\lambda)} + E. \end{aligned} \tag{16d}$$

From Eqs. (2), (3), (10c), (15a), (15b), and (16b), $r_i(i = 1, 2, 3, 4)$ can be derived as follows:

$$\begin{aligned} r_1^2 &= L^2/2 + X_o^2 + Y_o^2 + Z_o^2 \\ &\quad + L(l_1 x_m - l_2 y_m - X_o + Y_o) + \left(3l_2^2 - l_1^2\right)/4, \\ r_2^2 &= L^2/2 + X_o^2 + Y_o^2 + Z_o^2 \\ &\quad - L(l_1 x_l + l_2 y_l + X_o + Y_o) + \left(3l_1^2 - l_2^2\right)/4, \\ r_3^2 &= L^2/2 + X_o^2 + Y_o^2 + Z_o^2 \\ &\quad + L(l_2 y_l - l_1 x_l + X_o - Y_o) + \left(3l_1^2 - l_2^2\right)/4, \\ r_4^2 &= L^2/2 + X_o^2 + Y_o^2 + Z_o^2 \\ &\quad - L(l_2 y_m + l_1 x_m - X_o - Y_o) + \left(3l_2^2 - l_1^2\right)/4. \end{aligned} \tag{17}$$

From Eqs. (10c) and (16d), r_i $(i = 1, 2, 3, 4)$ can be represented by $(\alpha, \beta, \gamma, Z_o)$.

4.3. Solving active and constrained forces

On the basis of the force situation of a SPR-type active leg with a linear actuator (see Fig. 2), the force situation of the 2SPS+2SPR PM is determined (see Fig. 5b). From Eqs. (8), (9), and (13c), a formula for solving the active and constrained forces is expressed as

$$\begin{bmatrix} F_{a1} \\ F_{a2} \\ F_{a3} \\ F_{a4} \\ F_{c2} \\ F_{c3} \end{bmatrix} = -\left(\mathbf{J}_{6\times6}^{-1}\right)^{\mathrm{T}} \begin{bmatrix} \boldsymbol{F} \\ \boldsymbol{T} \end{bmatrix}, \quad \mathbf{J}_{6\times6} = \begin{bmatrix} \boldsymbol{\delta}_1^{\mathrm{T}} & (\boldsymbol{e}_1 \times \boldsymbol{\delta}_1)^{\mathrm{T}} \\ \boldsymbol{\delta}_2^{\mathrm{T}} & (\boldsymbol{e}_2 \times \boldsymbol{\delta}_2)^{\mathrm{T}} \\ \boldsymbol{\delta}_3^{\mathrm{T}} & (\boldsymbol{e}_3 \times \boldsymbol{\delta}_3)^{\mathrm{T}} \\ \boldsymbol{\delta}_4^{\mathrm{T}} & (\boldsymbol{e}_4 \times \boldsymbol{\delta}_4)^{\mathrm{T}} \\ \boldsymbol{c}_2^{\mathrm{T}} & (\boldsymbol{\rho}_2 \times \boldsymbol{c}_2)^{\mathrm{T}} \\ \boldsymbol{c}_3^{\mathrm{T}} & (\boldsymbol{\rho}_3 \times \boldsymbol{c}_3)^{\mathrm{T}} \end{bmatrix}. \tag{18}$$

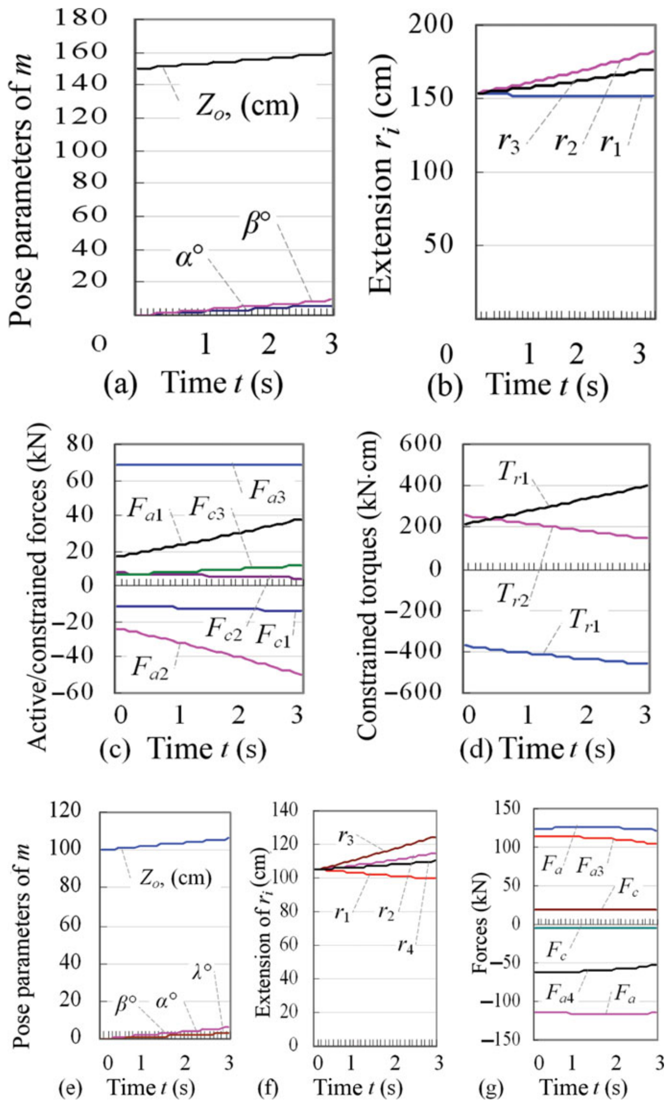

Fig. 5. (Colour online) The solved results of 3RRPRR and 2SPS+2SPR PMs.

The unit vector $\boldsymbol{\delta}_i$ of $r_i(i = 1, 2, 3, 4)$, the vector $\boldsymbol{e}_i$ of the line e_i, the unit vector $\boldsymbol{c}_i$ of constrained force $\boldsymbol{F}_{ci}$, and the arm vector $\boldsymbol{\rho}_i$ of $\boldsymbol{F}_{ci}$ to o can be solved as follows:

$$\begin{gathered} \boldsymbol{\delta}_i = \frac{\boldsymbol{a}_i - \boldsymbol{A}_i}{r_i}, \quad \boldsymbol{c}_2 = \frac{\boldsymbol{a}_1 - \boldsymbol{a}_3}{|\boldsymbol{a}_1 - \boldsymbol{a}_3|}, \quad \boldsymbol{c}_3 = \frac{\boldsymbol{a}_2 - \boldsymbol{a}_4}{|\boldsymbol{a}_2 - \boldsymbol{a}_4|}, \\ \boldsymbol{e}_i = \boldsymbol{o} - \boldsymbol{a}_i, \\ \boldsymbol{\rho}_2 = \boldsymbol{o} - \boldsymbol{A}_2, \quad \boldsymbol{\rho}_3 = \boldsymbol{o} - \boldsymbol{A}_3, \quad \boldsymbol{o} = \begin{bmatrix} X_o & Y_o & Z_o \end{bmatrix}^{\mathrm{T}}. \end{gathered} \tag{19}$$

All relevant items in Eq. (19) can be represented by $(\alpha, \beta, \gamma, Z_o)$ and can be solved using Eqs. (14a), (15a)–(15b), (16d), and (17).

5. Examples and Expandability of the Approach

5.1. Solved examples

Set workloads: $\boldsymbol{F} = [-20 - 30 - 60]^{\mathrm{T}}$kN, $\boldsymbol{T} = [-30 - 30\,100]^{\mathrm{T}}$ kN $\cdot$ cm. By means of relative analytic equations and Matlab, the active/constrained wrench of two PMs are solved (see Fig. 5). The solved results have been verified by their simulation mechanisms.

https://doi.org/10.1017/S0263574711000634 Published online by Cambridge University Press

In the 3RRPRR PM, when set $L = 120$, $l = 60$ cm, and given independent pose parameters (α, β, Z_o) versus time (see Fig. 5a). The extensions of active legs $r_i (i = 1, 2, 3)$ are solved (see Fig. 5b). The active forces F_{ai}, the constrained forces F_{ci}, and the constrained torques T_{ri} are solved (see Figs. 5c and 5d).

In the 2SPS+2SPR PM, when set $L = 100$, $l_1 = 60$, $l_2 = 50$ cm, and given the four independent pose parameters $(\alpha, \beta, \gamma, Z_o)$ versus time (see Fig. 5e); the extension of active legs $r_i (i = 1, 2, 3, 4)$ are solved (see Fig. 5f). The active forces $\boldsymbol{F}_{ai}$ and the constrained forces $\boldsymbol{T}_{ri}$ are solved (see Fig. 5g).

5.2. The expandability of proposed approach

In dynamics analysis of the limited-DOF PMs, when some formulae are derived for solving the Jacobian matrices and velocity/acceleration of the piston/cylinder in the legs of PMs, the formulae can be derived for solving the inertia wrenches/gravity of the various legs. After that, based on the statics Eq. (9) and Fig. 2 in Section 2.4, when the inertia wrenches/gravity of the legs and the friction loads of the joints are transformed into a part of the dynamic workload, the formulae may be derived for solving the dynamic workloads and the dynamic active/constrained wrench.

In elastic deformation analysis of the limited-DOF PMs, the force situations of some limited-DOF PMs can be analyzed, and the poses of the active/constrained wrench can be determined based on the statics equation (9) and Fig. 2 in Section 2.4. After that the elastic deformations of active/constrained legs in these PMs can be analyzed, and the compliance matrices of active/constrained legs can be derived. Finally, based on 6×6 Jacobina matrix in Eq. (9) and the compliance matrices of active/constrained legs, some total stiffness matrices and the elastic deformations of some limited-DOF PMs may be derived and analyzed.

6. Conclusions

A methodology is developed for unified statics analysis of some limited-DOF parallel kinematic machines PMs. A common force balanced equation and a unified 6×6 Jacobina matrix are derived. They can be used to solve the active/constrained wrench of the limited-dof PMs. The 21 types of accepted active legs with linear/rotational actuator are synthesized. Three common geometric constraints of the constrained wrench are determined and can be used to determine the poses of active/constrained wrench corresponding to the 21 different accepted active legs are determined. When these accepted active legs are used to synthesize various limited-DOF PMs, their active/constrained wrench can be solved.

This approach has been used to solve the active forces and constrained forces of a 3-DOF 3RRPRR PM and a 4-DOF 2SPS+2SPR PM. The solved results are verified by their simulation mechanisms.

The proposed approach is simple, intuition, and easy to be used to determine the poses of the various active/constrained wrench and to analyze unified statics of some limited-DOF PMs. It is provide foundations for analyses of the dynamics and the elastic deformation of various limited-DOF PMs.

Acknowledgments

The authors would like to acknowledge the financial support of the Key planned project of Hebei application foundation No. 11962127D.

References

1. S. B. Niku, *Introduction to Robotics Analysis, Systems, Applications* (Pearson Education, Inc., Publishing as Prentice Hall, and Publishing House of Electronics Industry, Beijing, China, 2004).
2. Z. Huang, L. F. Kong and Y. F. Fang, *Theory on Parallel Robotics and Control* (Machinery Industry Press, Beijing, China, 1997).
3. Y. Lu, B. Hu and P. L. Liu, "Kinematics and dynamics analyses of a parallel manipulator with three active legs and one passive leg by a virtual serial mechanism," *Multibody Syst. Dyn.* **17**(4), 229–241(2007).
4. Bh. Dasgupta and T. S. Mruthyunjaya, "A Newton-Euler formulation for the inverse dynamics of the Stewart platform manipulator," *Mech. Mach. Theory* **33**(8), 1135–1152 (1998).
5. L. W. Tsai, "Solving the inverse dynamics of a Stewart-Gough manipulator by the principle of virtual work," *ASME, J. Mech. Des.* **122**(1), 3–9 (2000).
6. J. Gallardo, J. M. Rico, A. Frisoli, D. Checcacci and M. Bergamasco "Dynamics of parallel manipulators by means of screw theory," *Mech. Mach. Theory* **38**(11), 1113–1131 (2003).
7. J. S. Dai and Z. Huang, "Harvey Lipkin. Mobility of over constrained Parallel Mechanisms," *ASME J. Mech. Des.* **128**(1), 220–229 (2006).
8. J. S. Zhao, W. Lu, F. Chu and Z. J. Feng, "The kinematics and statics of manipulators," *J. Mech. Eng. Sci. Proc. IMechE Part C* **223**(9), 2155–2166 (2009).
9. R. Di Gregorio, "Statics and singularity loci of the 3-UPU wrist," *IEEE Trans. Robot.* **20**(4), 630–635 (2004).
10. X. W. Kong and C. M. Gosselin, *Type Synthesis of Parallel Mechanisms* (Springer Tracts in Advanced Robotics, Heidelberg, 2007).
11. Y. Lu and B. Hu, "Unification and simplification of velocity/ acceleration of limited-dof parallel manipulators with linear active legs," *Mech. Mach. Theory* **43**(9), 1112–1128 (2008).
12. Y. Lu, "Using virtual work theory and CAD functionalities for solving driving force and driven force of spatial parallel manipulators," *Mech. Mach. Theory* **42**, 839–858 (2007).
13. Y. Lu and B. Hu, "Solving driving forces of 2(3-SPR) serial-parallel manipulator by CAD variation geometry approach," *ASME J. Mech. Des.* **128**(6), 1349–1351 (2006).
14. T. S. Zhao, J. S. Dai and Z. Huang, "Geometric analysis of overconstrained parallel manipulators with three and four degrees of freedom," *JSME Int. J. Ser. C, Mech. Syst. Mach. Elem. Manuf.* **45**(3), 730–740 (2002).
15. T. S. Zhao, J. S. Dai and Z. Huang, "Geometric synthesis of spatial parallel manipulators with fewer than six degrees of freedom," *Proc. Inst. Mech. Eng. J. Mech. Eng. Sci.C* **216**(12), 1175–1185 (2002).
16. K. Zhang, Y. Fang, J. S. Dai and H. Fang, "Geometry and constraint analysis of the 3-spherical kinematic chain based parallel mechanism," *ASME J. Mech. Robot.* **3**(2), 031014 (2010).
17. D. M. Gan, J. S. Dai and Q. Z. Liao, "Constraint analysis on mobility change in the metamorphic parallel mechanism," *Mech. Mach. Theory* **45**(12), 1864–1876 (2010).
18. W. Khalil and S. Guegan, "Inverse and direct dynamic modeling of Gough-Stewart robots," *IEEE Trans. Robot. Autom.* **20**(4), 754–762 (2004).
19. S. Ider, "Kemal Inverse dynamics of parallel manipulators in the presence of drive singularities," *Mech. Mach. Theory* **40**(5), 578–599 (2005).

20. M. Li, T. Huang, J. P. Mei, X. M. Zhao, D. G. Chetwynd and S. Jack Hu, "Dynamic Formulation and performance comparison of the 3-DOF modules of two Reconfigurable PM—The Tricept and the TriVariant," *ASME J. Mech. Des.* **127**(5), 1129–1136 (2005).
21. R. Andrea, S. Rosario and F. F. Xi, "Static balancing of parallel robots," *Mech. Mach. Theory* **40**(2), 191–202 (2005).
22. D. Bhaskar and T. S. Mruthyunjaya, "Force redundancy in parallel manipulators: theoretical and practical issues," *Mech. Mach. Theory* **33**(6), 727–742 (1998).
23. S. B. Nokleby, R. Fisher, R. P. Podhorodeski and F. Firmani, "Force capabilities of redundantly-actuated parallel manipulators," *Mech. Mach. Theory* **40**(5), 578–599 (2005).
24. D. Chakarov "Study of the passive compliance of parallel manipulators," *Mech. Mach. Theory* **34**(3), 373–389 (1999).
25. S. C. Wang, H. Hikita and H. Kubo, "Kinematics and dynamics of 6 degree-of-freedom fully parallel manipulator with elastic joints," *Mech. Mach. Theory* **38**, 439–461 (2003).